

RESEARCH ARTICLE

An Electroadhesive Paper Gripper With Application to a Document-Sorting Robot

HIDEAKI ITOH¹, TAKUYA OKAMOTO², HISAO FUKUMOTO¹, (Member, IEEE), AND HIROSHI WAKUYA³, (Member, IEEE)

¹Department of Electrical and Electronic Engineering, Faculty of Science and Engineering, Saga University, Saga 840-8502, Japan

²Electrical and Electronic Engineering Course, Graduate School of Science and Engineering, Saga University, Saga 840-8502, Japan

³Integrated Center for Educational Research and Development, Faculty of Education, Saga University, Saga 840-8502, Japan

Corresponding author: Hideaki Itoh (hideaki@cc.saga-u.ac.jp)

This work was supported in part by JSPS KAKENHI Grant Number JP 19K12157.

ABSTRACT Robotic process automation (RPA) is automating various job processes in many offices. However, most existing RPA systems automate only processes that are performed on computers. It is highly desirable to develop physical RPA systems that incorporate real robots to automate physical job processes. When developing physical RPA systems, handling paper is particularly important because many physical office jobs involve handling paper documents. However, it is not easy for robots to handle paper because paper is fragile. To address this issue, we propose an electroadhesive paper gripper in this study. The use of electroadhesion enables a robot to handle paper in a simple, non-destructive, and quiet manner. We provide (1) a mechanism for lifting a sheet of paper without accurate control of robot hands, (2) a mechanism for a small gripper to hold a large sheet of paper without bending it, and (3) a method for quickly releasing a sheet of paper. Furthermore, we apply the proposed paper gripper to a document-sorting robot. The robot that we have developed automatically arranges a given stack of paper documents in a predetermined order (e.g., alphabetical or numerical). Experimental results show the validity of the paper gripper and the sorting robot.

INDEX TERMS Automatic document-sorting robot, electroadhesive paper gripper, physical robots in offices, robotic process automation (RPA).

I. INTRODUCTION

Recently, robotic process automation (RPA) [1], [2], [3] has been introduced in many offices to automate various job processes, such as extracting data from PDF files, creating tables on spreadsheets, and writing emails. RPA reduces time-consuming manual labor, enabling office workers to spend their time on more productive work.

However, most existing RPA systems automate only computer-based processes. Physical processes that are not automated by RPA become bottlenecks when automating an entire job process. Therefore, it is highly desirable to develop physical RPA systems that incorporate real robots to automate physical job processes.

When developing such physical RPA systems, the ability of robots to handle paper is particularly important, because

The associate editor coordinating the review of this manuscript and approving it for publication was Yangmin Li.

many physical office jobs involve handling paper documents. However, it is not easy for robots to handle paper because paper is fragile. Rigid robot hands can be used to manipulate paper [4], [5], [6], but complex control of the robot hands is required. Roller-based paper feeding mechanisms, which are used in many office machines such as printers and document scanners, enable quick paper feed in fixed paper feed processes, but it is difficult for robots to use them to handle paper when flexibly automating various job processes; moreover, such mechanisms sometimes cause paper jams and damage important documents. Suction cups and vacuum pumps (Section II) can be used for sucking up a sheet of paper, but they are noisy and thus unsuitable for use in quiet office environments.

To address this issue, in this study, we propose a novel electroadhesive paper gripper. The basic structure of our gripper is the same as that of existing pad-based electroadhesive grippers [7], [8], [9], [10]; it consists of a pad

with embedded interdigital electrodes and a controller that applies high voltages to the electrodes. The pad adheres to a sheet of paper via electrostatic force when a high voltage is applied to the electrodes [7], [11], [12], [13]. Thus, the gripper enables a robot to grip a sheet of paper with a simple control of its hand. Also, the gripper is non-destructive in the sense that it does not damage the target paper via paper jams. Furthermore, the gripper makes no noise.

In this paper, we make the following contributions regarding the electroadhesive paper gripper. First, we provide a mechanism for a robot to lift a sheet of paper without accurate control of its hand. To lift a sheet of paper with an electroadhesive pad, the pad must be placed on the target sheet so that the pad can adhere to it. When the target sheet of paper is at the top of a stack of paper, the pad must be accurately positioned according to the height of the stack. In existing pad-based electroadhesive grippers [7], [8], [9], [10], such accurate positioning of the pad is required; the height of the stack needs to be measured with a certain sensor, and the pad needs to be positioned accordingly. To avoid this, in the present study, we use passive revolute and prismatic joints so that the pad automatically makes good contact with the target paper. Moreover, we study basic properties of the electroadhesion force that acts on stacked sheets of paper so that the gripper can grip only a single target sheet of paper at the top of a stack of paper.

Second, we provide a mechanism for a small gripper to hold a large sheet of paper without bending it. In fact, we made our pad smaller than half the size of a target sheet of paper. This enables the whole robot system to be small, which is desirable for the system to be used in offices. Conventional pad-based electroadhesive grippers [7], [8], [9], [10] can only hold a sheet of paper smaller than the pad; when the target sheet is larger than the pad, the pad adheres to only a part of the target sheet, and the remaining part of the sheet bends down. This risks the paper hitting the ground (or any other objects) and getting damaged. To avoid this, we separate our electroadhesive pad into two parts that can be slightly angled with respect to each other. With this structure, the target sheet of paper is slightly angled when it is lifted up by the pad. We show that this prevents the sheet of paper from bending down.

Third, we show that a simple method can be used to quickly release a sheet of paper. A drawback of using the electroadhesion force is its long release time [12], [14]. After turning off the voltage applied to the electrodes, the adhesion force lasts for a while owing to the remaining electric charges. This is problematic especially in our application because a sheet of paper is light and thus adheres to the pad for a long time (10 s or longer) after the voltage application is turned off. In the literature on electroadhesion, several methods have been proposed for quickly releasing the target object, including those that oscillate the applied voltage [8], [15], bend the electrodes [16], and vibrate the electrodes [17]. However, these methods require complex electric circuits or pad structures. In this paper, we show that a simple method

in which a reverse voltage is applied to the electrodes for a short period of time enables a quick release of a sheet of paper.

Last, as an example of a physical RPA system, we developed a document-sorting robot using our electroadhesive paper gripper. Here, document sorting means arranging a given stack of paper documents in a predetermined order (e.g., alphabetical or numerical). Such document sorting is a time-consuming, non-productive task that is undesirable for human workers to perform. Our developed robot automatically performs this task. To date, the sorting of an array of numbers stored in computer memory has been extensively studied in computer science (e.g., [18], [19], [20]), but the physical sorting of paper documents has rarely been studied.

The remainder of this paper is organized as follows. Section II discusses related work. Section III describes the electroadhesive paper gripper. Section IV describes the sorting robot. Section V presents our experimental results, and Section VI concludes the paper.

A preliminary version of this paper has been published in [21].

II. RELATED WORK

Electroadhesion has been used in many applications, including wall climbing [22], [23], perching [24], [25], sorting granular material mixture [26], and gripping objects [7], [8], [9], [10], [16], [27], but few studies have focused on handling paper documents. An exception is the automatic page-turning mechanism proposed by Lee et al. [28]. However, in their study, the target was a page in a book, and thus they did not need to consider the issues raised in the present paper. For example, each page could be easily released from the electroadhesive pad when the pad was moved away from the book.

Some existing general-purpose electroadhesive grippers have been used for gripping a sheet of paper. In [9], it was demonstrated that an electroadhesion robot gripper by Grabit Inc. could grip a sheet of paper. However, unlike ours, their gripper was larger than the target sheet of paper, and a large industrial robot was used to hold the gripper. In [27], a soft continuum manipulator with an electroadhesive pad was used to lift a sheet of paper. However, a PVC sheet had to be glued to the sheet of paper to prevent the paper from bending. In [16], it was shown that a non-pad-based electroadhesive gripper could grip a small sheet of paper, but the sheet of paper would bend down if it is larger.

Our gripper uses passive joints to automatically make good contact with a target sheet of paper on a stack of paper and to hold a large sheet of paper without bending it. Passive mechanisms have also been used in previous studies on robotic grippers. In [29], a three-fingered robot hand that can pick up a thin object lying on a smooth hard surface was developed, where a passive joint was used in a finger to make the finger automatically touch the hard surface. In [30], a three-fingered robot hand that can grasp spherical and cylindrical

objects was developed, where passive joints were used for the fingers to automatically switch between spherical and cylindrical grasps. Furthermore, various types of soft grippers (e.g., [16], [31]) have been developed using soft materials to create fingers that passively conform to target objects of various shapes. However, a mechanism for gripping a sheet of paper on a stack of paper has not been studied.

The mechanical part of our gripper is constructed by assembling modules such as LEGO pieces and plastic plates (Section III-B2). Such a modular approach has many advantages, including reconfigurability and low cost [32]. For example, our gripper can be easily reconfigured according to the size of the target sheet of paper. It can also be created inexpensively because each module costs only a few cents or dimes. Recently, modular methods have been extensively studied for constructing various structures such as flexure-based micro-positioning stages [33], [34] and cement-based civil engineering structures [35]. Designing each module and analyzing the overall performance [33], [34] are important areas of research even though they are beyond the scope of this study.

In Section V-A1, we study the electroadhesion force that acts on a stack of paper. In the literature, there have been studies on electroadhesion forces on other materials such as fabrics [36], aluminum plates and sandpaper samples [37], acrylic, glass, polycarbonate, and PET [38], and polylactic acid [10]. However, the force on a stack of paper has not been previously studied. A sheet of paper is a unique target for gripping in that it is very thin. When gripping a sheet of paper at the top of a stack of paper, it is important for the gripper not to grip the sheets of paper under the top one. Thus, we study not only the adhesion force that acts on the sheet of paper at the top of a stack of paper but also the force that acts on the sheets underneath. We note that, in this study, we focus on the adhesion force between the gripper and sheets of paper. The force will vary with different target materials.

In the present study, we use no sensor for the gripper. As shown in Section V-B, our gripper successfully lifts a sheet of paper over hundreds of times without using any sensors. However, it sometimes fails to lift a sheet of paper if, for example, we shorten the time of the high-voltage application to speed up the paper handling process. In such a case, we will be able to detect the failure by using a sensor such as a capacitive sensor [39] and a touch sensor [40]. If such a failure is detected, the robot will be able to retry lifting the target sheet of paper, although performing this is outside the scope of the present study.

Vacuum grippers that can grip objects using suction cups and vacuum pumps [41] are widely used in material-handling industries, and they can grip a sheet of paper as well [42], [43]. However, as mentioned in Section I, they make noise; the sound level of a typical quiet-type vacuum gripper is 50 dB or higher [43], [44]. In contrast, our electroadhesive gripper makes no sound at all, which is advantageous for use in quiet office environments.

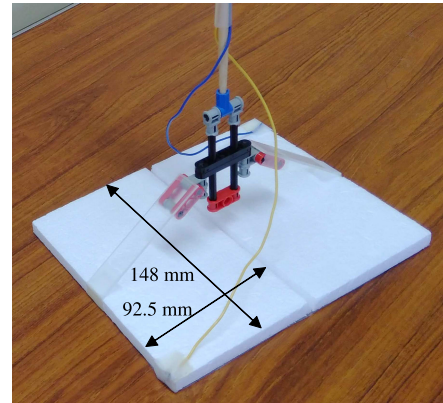


FIGURE 1. Top view of the electroadhesive pad.

III. ELECTROADHESIVE PAPER GRIPPER

As mentioned in Section I, our electroadhesive paper gripper consists of a pad with embedded interdigital electrodes and a controller that applies high voltages to the electrodes. The pad adheres to a sheet of paper when a high voltage is applied to the electrodes.

A. PAD

A top view of the pad is shown in Fig. 1. The pad consists of two 148 mm \times 92.5 mm rectangular flat panels that are connected to each other. In this study, we focus on handling A4 paper (297 mm \times 210 mm) because it is one of the most popular paper sizes in offices. The pad is made much smaller than A4 paper (it is smaller than half of A4 paper) so that the pad can be easily held and moved by a small robot (see Section IV).

Fig. 2(a) shows a cross-section of the pad. Electrodes made of aluminum (0.04-mm-thick aluminum foil, ON-3501, Onoue Manufacturing Co., Ltd.) are fixed under a substrate made of expanded polystyrene (10-mm-thick high-density styrene board, No. 165, Tamiya, Inc.). See Section III-B1 for its fabrication process. For insulation, the electrodes are covered by a dielectric material, namely sticky tape made of acetone (0.058-mm-thick Scotch mending tape, 3M Company). Here, aluminum foil was used as the electrodes because it can be easily cut into the interdigital shape. Expanded polystyrene was used as the substrate because it is lightweight. The substrate is 6 g, and the electrodes covered with the tape weigh 7 g. Acetone tape was used as the insulator because it has a high dielectric constant, which results in a strong adhesive force [7], [45], [46].

The rod shown at the top in Fig. 2(a) is a rigid body held by a robot hand. The substrate of the pad is hung from the rod via passive revolute and prismatic joints made of LEGO pieces (The Lego Group) and hanging plates made of plastic (1.7-mm-thick plastic plate, No. 128, Tamiya, Inc.). See Section III-B2 for the fabrication process. A side view of the pad shown in Fig. 2(b) illustrates the movements of those joints. The displacement of the prismatic joints, denoted by d in Fig. 2(a), can vary within a range of 0 to 4 cm.

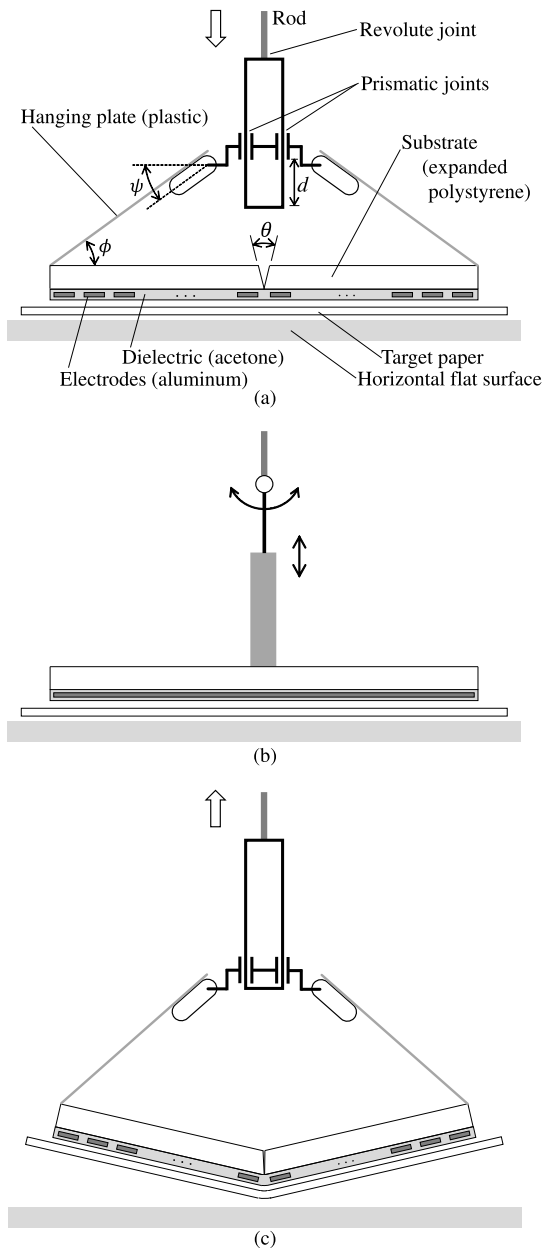


FIGURE 2. (a) Cross-section and (b) side view of the electroadhesive pad when the pad is put down onto a target sheet of paper. (c) Cross-section of the pad when it is lifted up. The two plates of the pad are slightly angled, and so is the target sheet of paper.

Those passive revolute and prismatic joints enable a robot to lift a sheet of paper without accurate control of the robot hand. The robot that is holding the rod in its hand only needs to put the pad down on a target sheet of paper. The passive joints automatically place the pad on the target sheet: The revolute joint makes the pad parallel to the target sheet even if the rod is tilted, and the prismatic joints adjust the vertical position of the pad (within the range of the displacement d) so that the pad makes good contact with the target sheet regardless of the height of the target. Once the pad is placed on the target, the robot can lift the target up after applying a high voltage to the electrodes (Section V-A1).

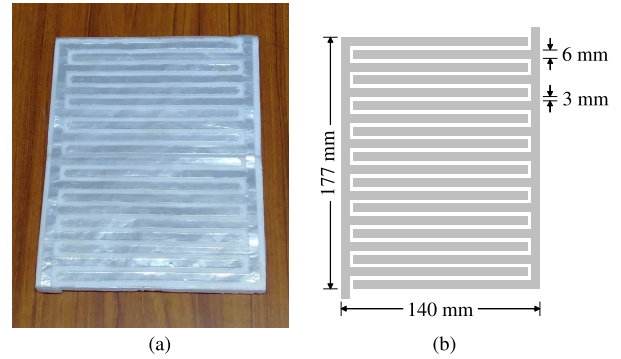


FIGURE 3. (a) Bottom view of the pads. (b) Shape of the interdigital electrodes.

We also propose a mechanism for holding a sheet of paper larger than the pad without bending it. As shown in Fig. 2(a), a wedge-shaped gap is created between the two panels constituting the pad, and passive revolute joints, whose angles are denoted by θ , ϕ , and ψ , are employed. Here, θ and ϕ are constrained to be non-negative angles. When the pad is put down on a target sheet of paper placed on a horizontal flat surface (Fig. 2(a)), the two panels are not angled, and thus the pad can easily adhere to the target. In this situation, the wedge angle θ is 30° . In contrast, when the pad is lifted up (Fig. 2(c)), the two panels are slightly angled with respect to each other. This makes the target sheet of paper slightly angled, which prevents it from bending down (see Section V-A2). In this situation, θ is 0° .

Fig. 3(a) shows the interdigital electrodes viewed from below the pad. The dull silver lines are the electrodes. Each line of the electrodes is 6 mm wide, and the gap between adjacent electrodes is 3 mm (Fig. 3(b)). The electrode area ($177 \text{ mm} \times 140 \text{ mm}$) is slightly smaller than that of the pad ($185 \text{ mm} \times 148 \text{ mm}$; Fig. 1) for the purpose of insulation. The electrode pattern is not the result of a rigorous optimization but was determined based on theoretical studies [11], [47], [48], [49] as well as trials and errors. Essentially, the narrower the gaps between the adjacent electrodes were, the stronger the adhesion force was. However, excessively narrow gaps caused electric discharges between the electrodes.

B. FABRICATION PROCESS

1) PAD

The pad was fabricated as follows. First, the electrode shape was drawn on a personal computer and printed on a sheet of paper using a standard laser printer. Next, the printed shape was placed on a piece of aluminum foil (Fig. 4(a)) and traced with a pencil so that it could be transferred onto the aluminum foil. Then, according to the transferred shape, the aluminum foil was cut with a box cutter to form the electrodes (Fig. 4(b)). Finally, as shown in Fig. 4(c), the electrodes were covered on both sides with acetone tape and fixed to the substrate with pieces of double-sided tape (NW-15, NICHIBAN Co., Ltd.). Also, sticky tape (Scotch mending tape, 3M Company) was applied to the substrate

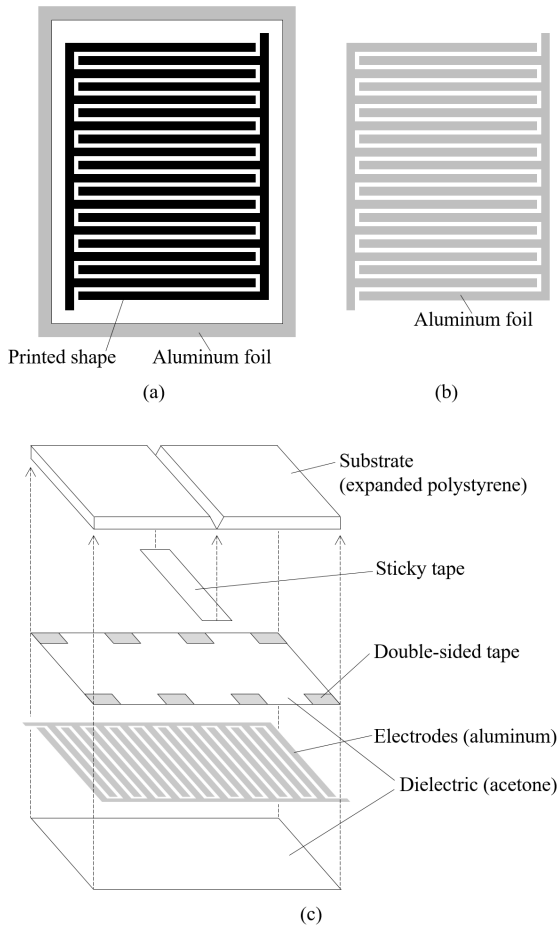


FIGURE 4. Fabrication process of the pad. (a) Target electrode shape printed on a sheet of paper was transferred onto aluminum foil. (b) The aluminum foil was cut to form the electrodes. (c) The electrodes were fixed to the substrate.

(Fig. 4(c)) to connect the two panels of the substrate and to form the joint of angle θ shown in Fig. 2(a).

2) MECHANICAL PART

The mechanical part of the gripper was fabricated as follows. First, LEGO pieces were assembled as shown in Fig. 5(a). The assembly was performed by putting the rod-shaped black pieces (called LEGO Technic Axles) through or into the holes of some other pieces along the cyan arrows shown in Fig. 5(a). The pieces shown in region A of Fig. 5(a) were assembled to make the same object as the one shown in region B (here, note that our gripper is bilaterally symmetric). The five yellow circles in Fig. 5(a) indicate holes in which the rod-shaped pieces could rotate. Those holes were used as the revolute, prismatic, and ψ joints shown in Fig. 2(a). The other holes were fixed joints; that is, the rod-shaped pieces could not rotate in them.

Next, the entire gripper structure was constructed as shown in Fig. 5(b). A rod was inserted into the topmost LEGO piece along arrow A. Two plastic hanging plates (85 mm \times 15 mm) were fixed with sticky tape (Scotch mending tape, 3M Company) to the wing-shaped parts as

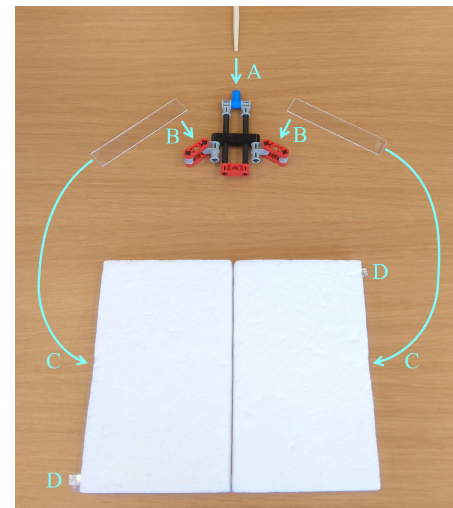
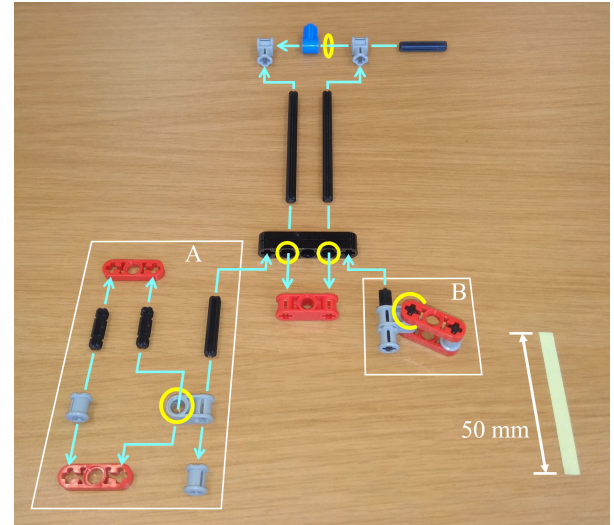


FIGURE 5. Fabrication process of the mechanical part of the gripper. (a) LEGO pieces were assembled. (b) The rod, hanging plates, pad, and power wires were connected. See text for details.

shown by arrows B. The other ends of the hanging plates were attached to the substrate of the pad with the sticky tape along arrows C so as to form the joints of angle ϕ shown in Fig. 2(a). Connecting power wires to the electrodes at points D completed the fabrication process. The outcome is shown in Fig. 1.

C. CONTROLLER CIRCUIT

To make the pad adhere to a target sheet of paper, we apply a high voltage to the electrodes. Additionally, we apply a reverse voltage to the electrodes to quickly release the target sheet of paper from the pad (see Section V-A3). Fig. 6 shows the circuit for controlling the voltage applied to the electrodes. The high-voltage generator in the circuit generates a high DC voltage V from a low DC voltage E . In our experiments of the sorting robot (Section V), E was 1.6 V supplied from a dry cell battery, and V was 1.8 kV.

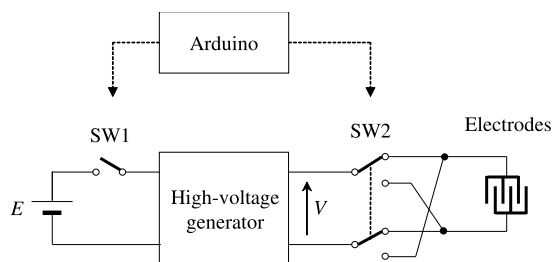


FIGURE 6. Controller circuit of the electroadhesive paper gripper.

The high-voltage generator consisted of a blocking oscillator that generated 620 V (peak to peak) AC from the DC input of $E = 1.6$ V and a three-stage Cockcroft–Walton multiplier that generated $V = 1.8$ kV DC from the 620 V AC.

The two switches in the circuit shown in Fig. 6, namely SW1 and SW2, are solid-state relays (SW1: TLP241A, Toshiba Cooperation; SW2: MOC3063, Isocom Components 2004 Ltd.) that are controlled by a single-board computer (Arduino Duemilanove). SW1 is turned off in the resting state. Before lifting up the target sheet of paper, SW1 is turned on and SW2 applies the high voltage V to the electrodes. The application of V continues while holding the sheet of paper. When releasing the sheet of paper, SW2 connects the high voltage V to the electrodes with the reverse polarity, and then, after a short period of time, SW1 is turned off. Here, the purpose of applying the reverse voltage is to eliminate charges that are remaining on the electrodes. If SW1 is not turned off shortly after SW2 has applied the reverse voltage, the electrodes adhere to the target sheet of paper again because excessive charges accumulate under the reverse polarity. The duration of the reverse voltage application was set to 30 ms based on the experiments described in Section V-A3.

IV. DOCUMENT-SORTING ROBOT

Using the electroadhesive paper gripper described in Section III, we developed a robot that can automatically sort a given stack of paper documents in a predetermined order. Fig. 7 shows an overview of the robot system.

A small humanoid robot (KHR-3HV Ver.2, Kondo Kagaku, Co., Ltd.) was used to move the electroadhesive pad. The pad was hung from the rigid rod (Fig. 2(a)), and the rod was fixed to the right hand of the robot. In front of the robot, three trays were placed so that the robot could place sheets of paper in them. These trays were useful for preventing the sheets of paper from going far away when they were released from the pad. A USB camera (ELP-USB13MAF-V75, Ailipu Technology Co., Ltd, resolution: 3840×2880 pixels) was placed above the central tray to capture the image of the paper document located in the tray. The robot, camera, and Arduino board (Fig. 6) were all connected to a desktop computer (CPU: Core i7 6700K, Intel Corporation), which ran our code that controlled the entire system. Our system was built on the Ubuntu OS using ROS [50]. The MoveIt motion planning library was used to control the robot to move the electroadhesive pad to desired locations.

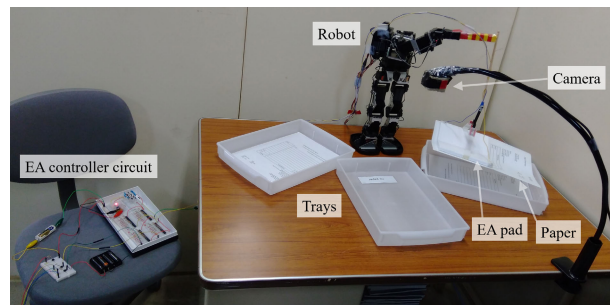


FIGURE 7. Overview of the document-sorting robot system. The electroadhesive (EA) pad and controller circuit shown in this picture are those presented in Figs. 1 and 6, respectively.

Moving a sheet of paper from one tray to another with our electroadhesive pad was easily accomplished with the following steps. First, the robot moves the pad to approximately 10 cm above the tray in which the target sheet of paper is placed. Next, the robot puts the pad down on the tray. The passive revolute and prismatic joints automatically ensure good contact between the pad and the target sheet of paper. Then, after applying a high voltage to the electrodes, the robot lifts the pad to 10 cm above the tray, moves the pad to 10 cm above the destination tray, and put it down on the destination tray. Finally, a reverse voltage is applied to the electrodes to release the sheet of paper.

In this study, we used a simple sorting algorithm. Here, we explain the algorithm using the example shown in Fig. 8. In this example, three sheets of paper are to be sorted in ascending numerical order based on the number written on each sheet, although our algorithm can be used to sort a larger number of sheets of paper and to arrange them in any type of order (e.g., alphabetical). We let the three trays that are placed in front of the robot be denoted by Trays A, B, and C, respectively (Fig. 8). We assume that all of the sheets of paper are initially placed in Tray B (Fig. 8(a)). The goal of the sorting task is to place all of them into Tray C in ascending numerical order (Fig. 8(e)).

The algorithm begins by recognizing the number written on every sheet of paper. Although the sheets of paper in Fig. 8 are drawn as if every number written on them is visible, in reality, only the number of the top sheet of paper is visible because the sheets of paper are stacked. To recognize the number written on every sheet of paper, the robot moves all the sheets of paper from Tray B to Tray A one by one (Fig. 8(b)). Before each sheet of paper is moved, an image of the top sheet of paper in Tray B is captured by the USB camera, and then the number written on the sheet is recognized by an open-source optical character recognition (OCR) program (Tesseract OCR). In the experiment described in Section V-B, we made our robot sort invoice documents. Fig. 9 shows an example image of a target invoice document captured by the USB camera. The OCR program recognized the number written after “INVOICE #” on each document.

A piece of paper with the words “no paper” written on it adheres to the bottom of Tray B (Fig. 8(b)). When the OCR

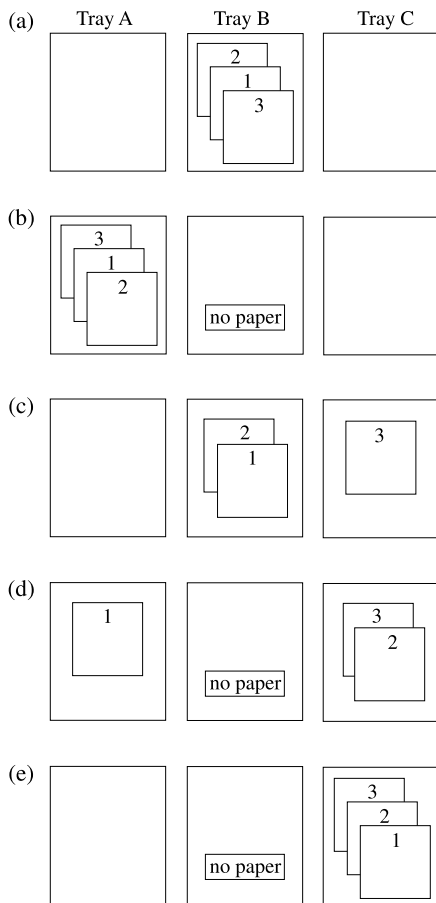


FIGURE 8. Example of document sorting. The sorting process proceeds from (a) to (e). See text for details.

program recognizes these words, the algorithm stops trying to handle a new sheet of paper in Tray B and starts sorting the sheets of paper in Tray A.

The algorithm traces the location (i.e., tray and order in stack) of each sheet of paper. Therefore, when all the sheets of paper have been moved to Tray A (Fig. 8(b)), the algorithm knows that all the sheets are located in Tray A, and it also knows the order in which the sheets of paper are stacked in Tray A. Given this knowledge, the algorithm can determine which sheet of paper should be moved to Tray C first. In Fig. 8(b), for example, the sheet of paper with the largest number (i.e., 3) is located at the bottom of the stack in Tray A. To move this sheet to Tray C, the algorithm moves all the sheets of paper above the target sheet of paper to Tray B, and then it moves the target sheet of paper to Tray C (Fig. 8(c)). This process is repeated until all the sheets of paper are moved to Tray C. In Fig. 8(c), for example, the next target is the sheet of paper with the second largest number (i.e., 2), which is located at the bottom of Tray B. Therefore, the sheet of paper located above the target sheet is moved to Tray A, and then the target sheet is moved to Tray C (Fig. 8(d)). The next target sheet is in Tray A and there are no other sheets of paper covering it. Therefore, the algorithm directly moves it to Tray C (Fig. 8(e)). This completes the sorting.

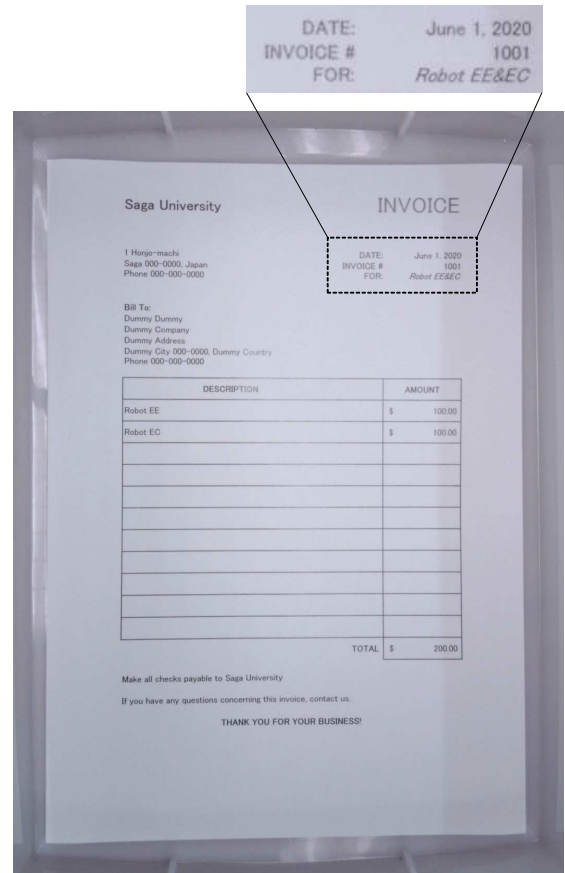


FIGURE 9. Example image of a target document captured by the USB camera. The number written after “INVOICE #”, which is “1001” in this example, was recognized by the OCR program and used for sorting.

The time required for the sorting task depends on how the given sheets of paper are initially arranged. In the worst case, the algorithm requires $N(N + 3)/2$ movements, where a movement means moving a sheet of paper from one tray to another, and N is the number of sheets of paper. The proof is as follows. The algorithm first requires N movements to move all the sheets of paper from Tray B to Tray A, and then it requires N movements at most to move the first target sheet of paper to Tray C, $N - 1$ movements at most to move the second target sheet of paper to Tray C, and so on. Therefore, the worst-case total number of movements is $N + \sum_{i=1}^N i = N + N(N + 1)/2 = N(N + 3)/2$. There may be better algorithms that require fewer movements than this, but finding such algorithms is beyond the scope of this paper.

V. EXPERIMENTS

A. HANDLING PAPER

1) GRIPPING PAPER

In this experiment, we studied the adhesion force generated by the electroadhesive pad. We need our paper gripper to grip only one sheet of paper at the top of a stack of paper; the gripper should not grip the other sheets under the top one. Thus, we studied the adhesion forces acting on the top

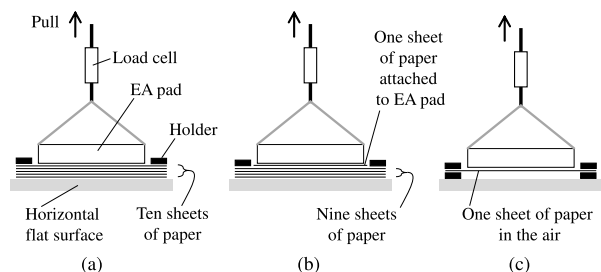


FIGURE 10. Experimental setups. The adhesion force generated by the electroadhesive (EA) pad was measured under three conditions: (a) ten-sheet, (b) nine-under-one, and (c) one-in-the-air.

sheet of paper and on the sheets under it. More specifically, we measured the electroadhesion normal forces under three conditions shown in Fig. 10. The experiments were conducted in an air-conditioned room with a temperature of $25.5 \pm 0.5^\circ\text{C}$ and a relative humidity of $32 \pm 1\%$.

The first condition (Fig. 10(a)), which we call the *ten-sheet* condition, was used to measure the overall adhesion force acting on a stack of paper. Under this condition, ten sheets of stacked paper were fixed on a horizontal flat surface with a holder. The holder was a 5.0-mm-thick, 1.1-kg-weight flat square board with a square hole in it. The size of the hole was made 168 mm \times 205 mm so that the electroadhesive pad could pass through it. The electroadhesive pad was placed on the sheets of paper and hung from a wire through a load cell (DST-5N, IMADA Co., Ltd.). After a high voltage was applied to the electrodes for a certain period of time, the pad was pulled up by a servo motor (KRS-2552RHV ICS, Kondo Kagaku, Co., Ltd.) at a slow speed of 6.6 mm/s, and the maximum tension before the pad was pulled away from the paper was measured with the load cell. The application of the high voltage was continued while the pad was being pulled up. Before each measurement of the maximum tension with the voltage application, we also measured the maximum tension without the voltage application, and we calculated the difference between those tensions to obtain the electroadhesion force generated by the voltage application.

The second condition (Fig. 10(b)), which we call the *nine-under-one* condition, was used to measure the adhesion force acting on sheets of paper stacked under the top sheet of paper. This condition was the same as the previous one except that nine sheets of paper, instead of ten, were fixed on a horizontal flat surface with the holder and that a sheet of paper, which was almost the same size as the pad, was attached to the pad with mending tape. (More precisely, the sheet of paper attached to the pad was 4 mm larger on each side than the pad and was attached to the pad by applying the mending tape to the 4-mm margins of the paper and the sides of the pad.) When the pad was pulled up, the sheet of paper attached to the pad was pulled up together with the pad. Thus, the adhesion force between the pad with the attached sheet of paper and the stack of paper under it was measured by the load cell.

The third condition (Fig. 10(c)), which we call the *one-in-the-air* condition, was used to measure the adhesion force

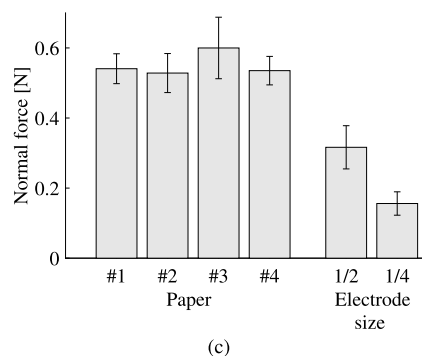
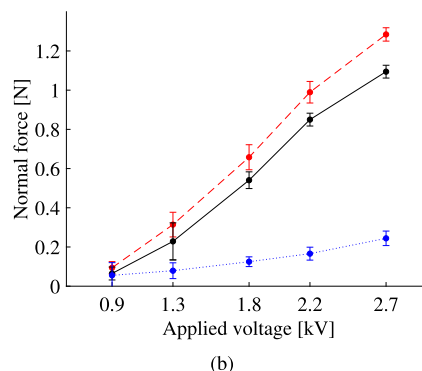
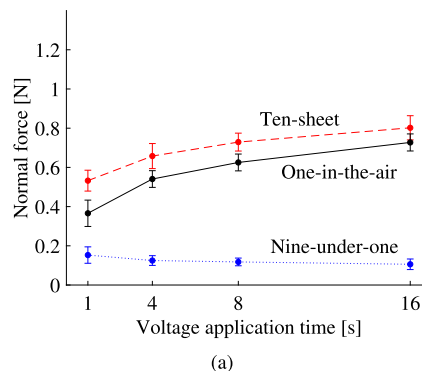


FIGURE 11. Electroadhesion normal forces measured (a) after a high voltage $V = 1.8$ kV was applied for various time lengths, (b) after various voltages were applied for 4 s, and (c) after a high voltage $V = 1.8$ kV was applied for 4 s with different kinds of paper (#1: plain, #2: recycled, #3: loose leaf, #4: colored) and electrode sizes. Each data point is the average of the results of ten experiments, and each error bar represents the standard deviation.

acting on a single sheet of paper under the pad. This condition was the same as the previous ones except that a sheet of paper was fixed in the air using the holders. The paper was placed 5 mm above the horizontal flat surface.

Fig. 11(a) shows the adhesion force after a high voltage $V = 1.8$ kV was applied to the electrodes for various time lengths (1, 4, 8, and 16 s). The red dashed, blue dotted, and black solid lines are the results in the ten-sheet, nine-under-one, and one-in-the-air conditions, respectively. We used plain office paper (64 g/m^2 KW copier paper, Japan Pulp & Paper Co., Ltd.) in all the experiments throughout this paper unless otherwise stated.

In Fig. 11(a), the results in the one-in-the-air condition (black line) show that the adhesion force acting on the

single sheet of paper under the pad increased as the voltage application time increased. In contrast, the results in the nine-under-one condition (blue line) show that the adhesion force acting on the sheets of paper under a sheet decreased as the voltage application time increased. Therefore, it is suggested that gripping only the top one sheet is easier when the voltage application time is longer. A possible reason for the negative slope of the blue line would be that, as the voltage application time increased, the top sheet of paper was drawn closer to the pad, creating a wider air gap between the top sheet and the sheets below it. We also note that the summation of the two forces in the one-in-the-air condition (black line) and nine-under-one condition (blue line) was approximately equal to the overall adhesion force indicated by the red line.

Fig. 11(b) shows the adhesion forces when the applied voltage V was changed. In this experiment, the voltage application time was fixed at 4 s. The results show that the adhesion forces in all of the three conditions increased as the applied voltage increased. We also note that, again in this experiment, the summation of the two forces in the one-in-the-air condition (black line) and nine-under-one condition (blue line) was approximately equal to the force in the ten-sheet condition (red line).

As shown in Fig. 11(a), when the voltage application time was 1 s, the adhesion force acting on the sheet of paper under the pad was around 0.37 N (≈ 38 gf). This force is strong enough to lift a sheet of A4 paper, which weighs approximately 4 to 8 g. Actually, when we used our pad in our robot system (Section V-B), it successfully lifted a sheet of paper in most cases. However, in rare cases, our pad failed to lift a sheet of paper due to disturbances such as airflow around the pad. To avoid such failures, we set the voltage application time to 4 s. With this setting, our pad successfully lifted a sheet of paper over hundreds of times (Section V-B).

As suggested in Fig. 11(a), the longer voltage application time of 4 s, compared with 1 s, was advantageous also for not lifting up the sheets of paper under the top sheet. When we used the pad in our robot system (Section V-B), we tried to shorten the voltage application time by increasing the applied voltage V , but when the applied voltage V was increased, the pad occasionally lifted two sheets of paper (i.e., the top sheet and the one beneath it).

Of course, a long voltage application time is disadvantageous when quick paper handling is required. As mentioned above, when the voltage application time was 1 s, our pad successfully lifted a sheet of paper in most cases. Such a short application time can be used if occasional failures are acceptable (e.g., if such a failure can be detected by a certain sensor and the robot can try re-gripping the target sheet).

We also measured the adhesion forces with four kinds of paper (Fig. 11(c) left), but there were no significant differences. The four kinds of paper that we used were as follows: #1: the plain office paper used in the experiments in Fig. 11(a)–(b); #2: recycled paper (66 g/m² PPC containing 70% or more recycled paper pulp, Daio Paper Corporation); #3: loose leaf paper (80 g/m² L1100, maruman

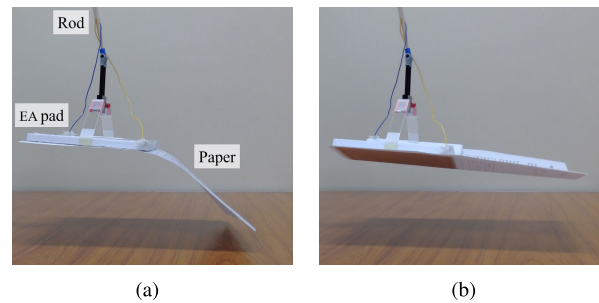


FIGURE 12. (a) Lifting a sheet of paper using the pad without the wedge results in bending of the sheet of paper. (b) Lifting a sheet of paper using the pad with the wedge enables holding the sheet without bending it.

Corporation); and #4: colored paper (128 g/m² NA-3419V, Nagatoya-shouten co., Ltd.).

Finally, we studied the adhesion forces with different electrode sizes (Fig. 11(c) right). For this experiment, we created electroadhesive pads with approximately half- and quarter-sized electrodes. The width (6 mm) and gaps (3 mm) of these electrodes were the same as those of the regular electrodes (Fig. 3(b)). The half-sized electrodes were created to be 86 mm \times 140 mm by reducing the number of fingers (i.e., the horizontally extended portions of the electrodes in Fig. 3(b)) from 20 to 10. The quarter-sized electrodes were created to be 86 mm \times 70 mm by halving the length of each finger of the half-sized electrodes. The results in Fig. 11(c) right show that the adhesion force was approximately proportional to the electrode size. Thus, although our pad was created to handle A4 paper, it will be possible for us to use electroadhesive pads of different sizes to handle paper of different sizes.

2) HOLDING PAPER

We tested whether our electroadhesive pad can hold an A4 sheet of paper without bending it. Fig. 12 shows the results. When there was no wedge between the plates constituting the pad, the plates were not angled, and the sheet of paper bent down (Fig. 12(a)). In contrast, when there was a wedge between the plates as shown in Fig. 2(a), the plates were slightly angled with respect to each other, and thus, two halves of the sheet of paper were slightly angled with respect to each other. This prevented the sheet from bending down (Fig. 12(b)). These results show that our mechanism (Section III-A) is effective for allowing the pad to hold a sheet of paper larger than the pad without bending it.

3) RELEASING PAPER

We also tested whether a sheet of paper can be quickly released by the application of a reverse voltage. In this experiment, we first placed the pad on a sheet of paper placed on a flat surface and then applied the high voltage V ($=1.8$ kV) to the electrodes for 10 s to make the pad adhere to the sheet. Here, a rather long voltage application time of 10 s was used to make sure that adhesion was firmly established. Then, we applied the reverse voltage for a period of time T . Finally, we cut off the voltage and observed whether the sheet

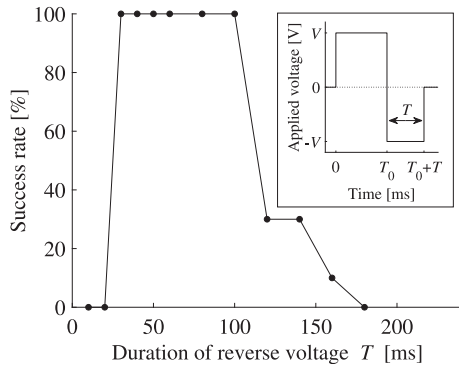


FIGURE 13. Success rate of releasing a sheet of paper versus the duration of the application of a reverse voltage. Each point is the result of ten experiments. The inset shows the temporal change in the voltage applied to the electrodes, where $T_0 = 10 \times 10^{-3}$ ms and $V = 1.8$ kV.

of paper was released. For each value of T , we performed the same experiment ten times and calculated the rate at which the sheet of paper was successfully released. The results (Fig. 13) show that the success rate is 100% when T is between 30 and 100 ms. Based on these results, we set T to 30 ms in the subsequent experiments.

B. SORTING DOCUMENTS

In this experiment, we had our robot perform a sorting task. First, we made the robot sort three invoice documents. An example invoice document is shown in Fig. 9. Each of the three documents had a different invoice number written on it. The three documents were initially arranged as shown in Fig. 8(a). Thus, the robot had to perform the sorting task in the same way as shown in Fig. 8. Fig. 14 shows how our robot performed the first operation of the task, i.e., the operation of moving the top sheet of paper in Tray B to Tray A. After this movement, the robot successfully continued performing the sorting task in the same way as shown in Fig. 8. A video of the entire sorting process is provided as supplementary material.

The video also shows that the electroadhesive pad made no noise. Although some noise was made by the servo motors of the robot, it can be reduced by replacing the servo motors with quieter ones.

Next, we made the robot sort different numbers of documents. Let N denote the number of documents. The documents were initially stacked in Tray B in the order that required the worst-case number of movements, i.e., $N(N + 3)/2$ (see Section IV), to complete the sorting. The dots in Fig. 15 indicate the time required by the robot to complete the sorting (right vertical axis) for various values of N (horizontal axis). The solid line in Fig. 15 shows the theoretical worst-case number of movements, i.e., $N(N + 3)/2$, required to complete the sorting (left vertical axis). The trend of the time spent on sorting (the dots in Fig. 15) well matches that of the number of movements (the solid line in Fig. 15), meaning that the total time was largely determined by the number of movements. Here, the total time includes the time for the OCR, but the OCR time was negligible because it required only approximately 1 s per document.

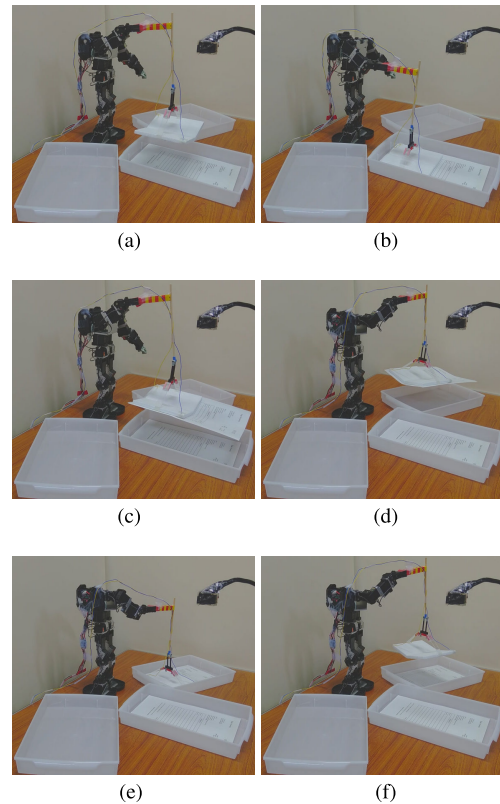


FIGURE 14. Photographs of the robot sorting paper documents. Time flows from (a) to (f). In this figure, the robot is moving the top sheet of paper in Tray B to Tray A. A video of the entire sorting process is provided as supplementary material.

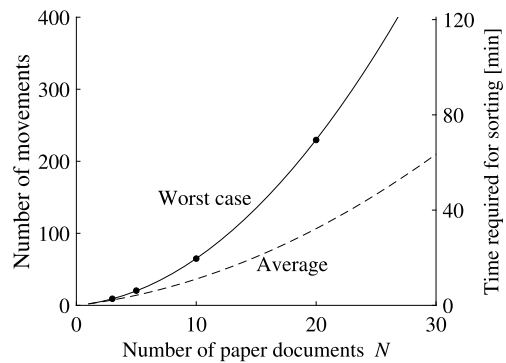


FIGURE 15. The solid and broken lines indicate the worst-case and average number of movements (left vertical axis) required for sorting N sheets of paper, respectively. The dots show the actual time (right vertical axis) spent by the robot to complete the sorting task that required the worst-case number of movements.

A disadvantage of the current robot system is that it requires a long time to complete the sorting. For example, it required approximately 70 minutes to sort 20 documents in the worst case (Fig. 15). However, the sorting is performed automatically with no human labor, and there are methods for speeding up sorting (see Section VI).

The broken line in Fig. 15 shows the average number of movements (left vertical axis) required to complete the

sorting task. The average number of movements for each N was estimated through 10^6 computer simulations, in each of which the initial arrangement of target documents was randomly determined with a uniform probability distribution. The results show that the average number of movements is approximately half of the worst-case number. Thus, it is expected that our robot can, on average, complete the sorting task in approximately half the time indicated by the dots in Fig. 15.

VI. CONCLUSION

In this paper, we have presented an electroadhesive paper gripper and a document-sorting robot. The paper gripper enables a robot to handle paper in a simple, non-destructive, and quiet manner. We have provided methods for lifting a sheet of paper without accurate control of robot hands, for a small gripper to hold a large sheet of paper without bending it, and for quickly releasing it. The document-sorting robot can automatically sort sheets of paper in a predetermined order.

An important future issue is to speed up the sorting process. During sorting, most of the time was spent moving the sheets of paper from one tray to another (Section V-B). The sorting time can be reduced by, for example, shortening the time in which we apply the high voltage before lifting each sheet of paper. We applied the high voltage for 4 s in our experiments, but less than 1 s is enough in most cases (Section V-A). If the voltage application time is shortened, the robot will occasionally fail to lift the target. However, it should be possible to detect such failures with some kind of sensor (Section II) and make the robot redo the lifting when a failure occurs. Another way to reduce the sorting time is to use more than three trays. As mentioned in Section IV, our sorting algorithm requires $N(N + 3)/2$ movements in the worst case, where N is the number of documents. The number of movements decreases if more than three trays are available. For example, if there are $N + 1$ trays available, the number of movements is reduced to $2N$, which is achieved by first moving each of the target N documents placed in the initial tray to N different trays and then moving the documents back to the original tray in a specified order. To use many trays, we could use a mobile robot that moves around to deliver a sheet of paper from one tray to another.

Another important future issue is to theoretically analyze the electroadhesion forces that act on stacked sheets of paper. In this study, we have empirically investigated the electroadhesion force that acts on the top sheet of paper as well as the force that acts on the sheets underneath. Theoretical analysis of those forces may enable us to design a gripper with improved performance in gripping only the top sheet of paper.

Yet another important future issue is to use the electroadhesive paper gripper in other RPA applications than document sorting. There are many time-consuming office jobs that are worth automating, such as sorting documents into categories, scanning paper documents of different sizes, and finding an important document from a pile of documents.

REFERENCES

- [1] W. M. P. Van Der Aalst, M. Bichler, and A. Heinzl, "Robotic process automation," *Bus. Inf. Syst. Eng.*, vol. 60, no. 4, pp. 269–272, Aug. 2018.
- [2] B. Vajgel, P. L. P. Corrêa, T. T. De Sousa, R. V. E. Quille, J. A. R. Bedoya, G. M. D. Almeida, L. V. L. Filgueiras, V. R. S. Demuner, and D. Mollica, "Development of intelligent robotic process automation: A utility case study in Brazil," *IEEE Access*, vol. 9, pp. 71222–71235, 2021.
- [3] R. Plattfaut, V. Borghoff, M. Godefroid, J. Koch, M. Trampler, and A. Coners, "The critical success factors for robotic process automation," *Comput. Ind.*, vol. 138, Jun. 2022, Art. no. 103646.
- [4] A. Namiki and S. Yokosawa, "Robotic origami folding with dynamic motion primitives," in *Proc. IEEE/RSJ Int. Conf. Intell. Robots Syst. (IROS)*, Hamburg, Germany, Sep. 2015, pp. 5623–5628.
- [5] J. Sanchez, J.-A. Corrales, B.-C. Bouzgarrou, and Y. Mezouar, "Robotic manipulation and sensing of deformable objects in domestic and industrial applications: A survey," *Int. J. Robot. Res.*, vol. 37, no. 7, pp. 688–716, Jun. 2018.
- [6] A. Namiki and S. Yokosawa, "Origami folding by multifingered hands with motion primitives," *Cyborg Bionic Syst.*, vol. 2021, May 2021, Art. no. 9851834.
- [7] R. P. Krape, "Applications study of electroadhesive devices," Chrysler Corp. Space Division, New Orleans, LA, USA, Tech. Rep. NASA CR-1211, 1968.
- [8] C. Brecher, F. Emonts, B. Ozolin, and R. Schares, "Handling of preforms and prepregs for mass production of composites," in *Proc. 19th Int. Conf. Composite Mater. (ICCM)*, Montréal, QC, Canada, 2013, pp. 4085–4093. (Apr. 24, 2014). *Grabit Electroadhesion Robot Gripper—Single Sheet Paper*. Grabit Inc., Sunnyvale, CA, USA. Accessed: Oct. 4, 2022. [Online]. Available: <https://www.youtube.com/watch?v=RXILgK96eOE>
- [10] J. D. West, J. Mici, J. F. Jaquith, and H. Lipson, "Design and optimization of millimeter-scale electroadhesive grippers," *J. Phys. D, Appl. Phys.*, vol. 53, no. 43, Aug. 2020, Art. no. 435302.
- [11] C. Cao, X. Sun, Y. Fang, Q.-H. Qin, A. Yu, and X.-Q. Feng, "Theoretical model and design of electroadhesive pad with interdigitated electrodes," *Mater. Des.*, vol. 89, pp. 485–491, Jan. 2016.
- [12] J. Guo, J. Leng, and J. Rossiter, "Electroadhesion technologies for robotics: A comprehensive review," *IEEE Trans. Robot.*, vol. 36, no. 2, pp. 313–327, Apr. 2020.
- [13] P. Rajagopalan, M. Muthu, Y. Liu, J. Luo, X. Wang, and C. Wan, "Advancement of electroadhesion technology for intelligent and self-reliant robotic applications," *Adv. Intell. Syst.*, vol. 4, no. 7, Jul. 2022, Art. no. 2200064.
- [14] C. Cao, X. Gao, J. Guo, and A. Conn, "De-electroadhesion of flexible and lightweight materials: An experimental study," *Appl. Sci.*, vol. 9, no. 14, p. 2796, Jul. 2019.
- [15] C. M. Horwitz, "Electrostatic chuck with improved release," U.S. Patent 5 325 261, Jun. 28, 1994.
- [16] J. Shintake, V. Cacucciolo, D. Floreano, and H. Shea, "Soft robotic grippers," *Adv. Mater.*, vol. 30, no. 29, Jul. 2018, Art. no. 1707035.
- [17] X. Gao, C. Cao, J. Guo, and A. Conn, "Elastic electroadhesion with rapid release by integrated resonant vibration," *Adv. Mater. Technol.*, vol. 4, no. 1, Jan. 2019, Art. no. 1800378.
- [18] C. A. Hoare, "Quicksort," *Comput. J.*, vol. 5, no. 1, pp. 10–16, Jan. 1962.
- [19] D. P. Singh, I. Joshi, and J. Choudhary, "Survey of GPU based sorting algorithms," *Int. J. Parallel Program.*, vol. 46, no. 6, pp. 1017–1034, Dec. 2018.
- [20] S. S. Moghaddam and K. S. Moghaddam, "A general framework for sorting large data sets using independent subarrays of approximately equal length," *IEEE Access*, vol. 10, pp. 11584–11607, 2022.
- [21] T. Okamoto, H. Itoh, H. Fukumoto, and H. Wakuya, "Developing a paper sorting robot for physical RPA," in *Proc. 26th Int. Symp. Artif. Life Robot. (AROB)*, 2021, pp. 206–210.
- [22] A. Yamamoto, T. Nakashima, and T. Higuchi, "Wall climbing mechanisms using electrostatic attraction generated by flexible electrodes," in *Proc. Int. Symp. Micro-Nanomechatron. Human Sci.*, Nagoya, Japan, Nov. 2007, pp. 389–394.
- [23] G. Gu, J. Zou, R. Zhao, X. Zhao, and X. Zhu, "Soft wall-climbing robots," *Sci. Robot.*, vol. 3, no. 25, Dec. 2018, Art. no. eaat2874.
- [24] M. A. Graule, P. Chirattananon, S. B. Fuller, N. T. Jafferis, K. Y. Ma, M. Spenko, R. Kornbluh, and R. J. Wood, "Perching and takeoff of a robotic insect on overhangs using switchable electrostatic adhesion," *Science*, vol. 352, no. 6288, pp. 978–982, May 2016.

- [25] S. Park, D. S. Drew, S. Follmer, and J. Rivas-Davila, "Lightweight high voltage generator for untethered electroadhesive perching of micro air vehicles," *IEEE Robot. Autom. Lett.*, vol. 5, no. 3, pp. 4485–4492, Jul. 2020.
- [26] H. Louati, N. Zouzou, A. Tilmatine, A. Zouaghi, and R. Ouiddir, "Experimental investigation of an electrostatic adhesion device used for metal/polymer granular mixture sorting," *Powder Technol.*, vol. 391, pp. 301–310, Oct. 2021.
- [27] C. Xiang, J. Guo, and J. Rossiter, "ContinuumEA: A soft continuum electroadhesive manipulator," in *Proc. IEEE Int. Conf. Robot. Biomimetics (ROBIO)*, Kuala Lumpur, Malaysia, Dec. 2018, pp. 2473–2478.
- [28] J. Lee, W. Jeon, Y. Cha, and H. Yang, "Automatic page-turning mechanism with near-field electroadhesive force for linearly correctable imaging," in *Proc. IEEE/RSJ Int. Conf. Intell. Robots Syst. (IROS)*, Vancouver, BC, Canada, Sep. 2017, pp. 279–285.
- [29] V. Babin, D. St-Onge, and C. Gosselin, "Stable and repeatable grasping of flat objects on hard surfaces using passive and epicyclic mechanisms," *Robot. Comput.-Integr. Manuf.*, vol. 55, pp. 1–10, Feb. 2019.
- [30] S. B. Backus and A. M. Dollar, "An adaptive three-fingered prismatic gripper with passive rotational joints," *IEEE Robot. Autom. Lett.*, vol. 1, no. 2, pp. 668–675, Jul. 2016.
- [31] W. Xu, H. Zhang, H. Yuan, and B. Liang, "A compliant adaptive gripper and its intrinsic force sensing method," *IEEE Trans. Robot.*, vol. 37, no. 5, pp. 1584–1603, Oct. 2021.
- [32] A. Brunete, A. Ranganath, S. Segovia, J. P. De Frutos, M. Hernando, and E. Gambao, "Current trends in reconfigurable modular robots design," *Int. J. Adv. Robotic Syst.*, vol. 14, no. 3, May 2017, Art. no. 1729881417710457.
- [33] B. Ding, Z. Yang, and Y. Li, "Design of flexure-based modular architecture micro-positioning stage," *Microsyst. Technol.*, vol. 26, no. 9, pp. 2893–2901, Sep. 2020.
- [34] S. Liao, B. Ding, and Y. Li, "Design, assembly, and simulation of flexure-based modular micro-positioning stages," *Mach.*, vol. 10, no. 6, May 2022, Art. no. 421.
- [35] R. Barhmat, S. Mahjoubi, V. C. Li, and Y. Bao, "Lego-inspired reconfigurable modular blocks for automated construction of engineering structures," *Autom. Constr.*, vol. 139, Jul. 2022, Art. no. 104323.
- [36] G. J. Monkman, P. M. Taylor, and G. J. Farnworth, "Principles of electroadhesion in clothing robotics," *Int. J. Clothing Sci. Technol.*, vol. 1, no. 3, pp. 14–20, Mar. 1989.
- [37] J. Guo, M. Taylor, T. Bamber, M. Chamberlain, L. Justham, and M. Jackson, "Investigation of relationship between interfacial electroadhesive force and surface texture," *J. Phys. D, Appl. Phys.*, vol. 49, no. 3, Dec. 2015, Art. no. 035303.
- [38] J. Guo, T. Bamber, J. Petzing, L. Justham, and M. Jackson, "Experimental study of relationship between interfacial electroadhesive force and applied voltage for different substrate materials," *Appl. Phys. Lett.*, vol. 110, no. 5, Jan. 2017, Art. no. 051602.
- [39] J. Guo, T. Bamber, Y. Zhao, M. Chamberlain, L. Justham, and M. Jackson, "Toward adaptive and intelligent electroadhesives for robotic material handling," *IEEE Robot. Autom. Lett.*, vol. 2, no. 2, pp. 538–545, Apr. 2017.
- [40] J. Guo, K. Elgeneidy, C. Xiang, N. Lohse, L. Justham, and J. Rossiter, "Soft pneumatic grippers embedded with stretchable electroadhesion," *Smart Mater. Struct.*, vol. 27, no. 5, Mar. 2018, Art. no. 055006.
- [41] G. Mantriota, "Theoretical model of the grasp with vacuum gripper," *Mechanism Mach. Theory*, vol. 42, no. 1, pp. 2–17, Jan. 2007.
- [42] S. Faibish, H. Bacakoglu, and A. A. Goldenberg, "An experimental system for automated paper recycling," in *Experimental Robotics V (Lecture Notes in Control and Information Sciences)*, vol. 232, A. Casals and A. T. De Almeida, Eds. Berlin, Germany: Springer, 1998, pp. 361–372. (Sep. 15, 2017). *Handling Paper Discs With Vacuum—Piab*. Piab AB, Täby, Sweden. Accessed: Oct. 4, 2022. [Online]. Available: <https://www.youtube.com/watch?v=FT7NwbXyM7Q>
- [44] E. Papadakis, F. Raptopoulos, M. Koskinopoulos, and M. Maniadakis, "On the use of vacuum technology for applied robotic systems," in *Proc. 6th Int. Conf. Mechatronics Robot. Eng. (ICMRE)*, Barcelona, Spain, Feb. 2020, pp. 73–77.
- [45] D. Ruffatto, A. Parness, and M. Spenko, "Improving controllable adhesion on both rough and smooth surfaces with a hybrid electrostatic/gecko-like adhesive," *J. Roy. Soc. Interface*, vol. 11, no. 93, Apr. 2014, Art. no. 20131089.
- [46] H. Lim, G. Hwang, K.-U. Kyung, and B.-J. Kim, "Improved electroadhesive force by using fumed alumina/PDMS composites," *Smart Mater. Struct.*, vol. 30, no. 3, Feb. 2021, Art. no. 035007.
- [47] J. Guo, T. Bamber, M. Chamberlain, L. Justham, and M. Jackson, "Optimization and experimental verification of coplanar interdigital electroadhesives," *J. Phys. D, Appl. Phys.*, vol. 49, no. 41, Sep. 2016, Art. no. 415304.
- [48] K. Choi, Y. Chan Kim, H. Sun, S.-H. Kim, J. W. Yoo, I.-K. Park, P.-C. Lee, H. J. Choi, H. R. Choi, T. Kim, J. Suhr, Y. K. Lee, and J.-D. Nam, "Quantitative electrode design modeling of an electroadhesive lifting device based on the localized charge distribution and interfacial polarization of different objects," *ACS Omega*, vol. 4, no. 5, pp. 7994–8000, May 2019.
- [49] J.-H. Kim, S.-H. Kang, and S. Cho, "Shape design optimization of interdigitated electrodes for maximal electro-adhesion forces," *Structural Multidisciplinary Optim.*, vol. 61, no. 5, pp. 1843–1855, May 2020.
- [50] M. Quigley, B. Gerkey, K. Conley, J. Faust, T. Foote, J. Leibs, E. Berger, R. Wheeler, and A. Ng, "ROS: An open-source Robot Operating System," in *Proc. ICRA Workshop Open Source Softw.*, Kobe, Japan, 2009, pp. 1–6.



HIDEAKI ITOH received the B.E., M.E., and D.E. degrees from the University of Tokyo, Tokyo, Japan, in 1997, 1999, and 2002, respectively. He was a Research Associate and an Assistant Professor at Tokyo Institute of Technology, Kanagawa, Japan. He joined Saga University, Saga, Japan, in 2009, where he has been a Professor since 2022. His research interests include electroadhesion and robotics.



TAKUYA OKAMOTO received the B.E. and M.E. degrees from Saga University, Saga, Japan, in 2020 and 2022, respectively. He is currently working with NEC Corporation. His research interests include robotics and artificial intelligence.



HISAO FUKUMOTO (Member, IEEE) received the B.E., M.E., and D.E. degrees from Saga University, Saga, Japan, in 1997, 1999, and 2002, respectively. In 2002, he joined Saga University, where he has been an Associate Professor since 2018. His research interests include image processing, signal processing, and higher education on engineering based on advanced computational engineering.



HIROSHI WAKUYA (Member, IEEE) received the B.E. degree from Kyushu Institute of Technology, Kitakyushu, Japan, in 1989, and the M.E. and D.E. degrees from Tohoku University, Sendai, Japan, in 1991 and 1994, respectively. In 1994, he joined Saga University, Saga, Japan, where he has been a Professor since 2021. His research interests include biomedical engineering and soft computing.

...